Synthesis, Characterization and Liquid Phase Oxidation of Cyclohexane with Hydrogen Peroxide over Oxovanadium(IV) Schiff-base Tetradendate Complex Covalently Anchored to Multi-Wall Carbon Nanotubes (MWNTs)

Masoud Salavati-Niasari* **and Mehdi Bazarganipour†**

*Institute of Nano Science and Nano Technology and Department of Chemistry, Faculty of Science, University of Kashan, Kashan, I.R. Iran. *E-mail: Salavati@kashanu.ac.ir*
†Department of Chemistry, Faculty of Science, University of Kashan, Kashan, I.R. Iran
Received November 18, 2008, Accepted January 5, 2009

The chemical modification of multi-wall carbon nanotubes (MWNTs) is an emerging area in material science. In the present study, hydroxyl functionalized oxovanadium(IV) Schiff-base; *N,N′*-bis(4-hydroxysalicylidene)-ethylene-1, 2-diamineoxovanadium(IV), [VO((OH)$_2$-salen)]; has been covalently anchored on modified MWNTs. The new modified MWNTs ([VO((OH)$_2$-salen)]-MWNTs]) have been characterized by transmission electron microscopy (TEM), X-ray diffraction (XRD), X-ray photoelectron (XPS), UV-Vis, Diffuse reflectance (DRS), FT-IR spectroscopy and elemental analysis. The analytical data indicated a composition corresponding to the mononuclear complex of tetradentate Schiff-base ligand. The characterization of the data showed the absence of extraneous complex, retention of MWNTs and covalently anchored on modified MWNTs. Liquid-phase oxidation of cyclohexane with H_2O_2 to a mixture of cyclohexanone, cyclohexanol and cyclohexane-1,2-diol in CH_3CN have been reported using oxovanadium(IV) Schiff-base complex covalently anchored on modified MWNTs as catalysts. This catalyst is more selective toward cyclohexanol formation.

Key Words: Multi-wall carbon nanotubes, Oxovanadium(IV), Heterogeneous catalyst, Oxidation of cyclohexane

Introduction

Since the discovery of carbon nanotubes (CNTs) in 1991,[1] many potential applications have been suggested due to their extraordinary mechanical[2-5] and electronic properties.[6-9] CNTs have a narrow distribution size, highly accessible surface area, low resistivity and high stability. Considerable theoretical and experimental investigations on their novel structure and applications have been carried out.[1-10] At present, CNTs have been produced primarily by arc discharge,[11] laser ablation,[12] and catalyzed chemical vapor deposition (CVD).[13] However, several technical challenges need to be overcome before the extraordinary properties of these unique materials can be fully utilized. For example, the produced CNTs are typically bound into intertwined bundles that exhibit very low solubility in either water or organic solvents. Several approaches have been investigated to improve dispersion and solubility of nanotubes, such as milling,[13,14] ultrasonication,[15] and high-shear-flow mixing,[16] combined with the addition of surfactants and dispersing agents.[17,18] Another approach that has opened a large number of research opportunities and potential applications is chemical functionalization.

Functionalization of carbon nanotubes is an effective way to enhance the physical properties and improve the solubility. however, the aromatic character of nanotubes restricts the possible addition reactions. The functionalization of carbon nanotubes may extend the range of their potential applications. The electric properties of CNTs can be modified using chemical functionalization and the contact resistance between the interconnected tubes can be reduced by chemically binding functional groups. Suitable functionalization enables the linking of individual carbon nanotubes to form complex networks for nanoscale electronic circuits.[19] The functionalization solubilizes the nanotubes in a variety of solvents,[20,21] allows chemical manipulations and improves the dispersion in composite applications. In nanocomposites, the functional groups attached to the walls of CNTs can form strong chemical bonds with the surrounding polymer matrix, increasing the binding force between the nanotube and polymer.[22,23]

Some of the functionalization approaches previously reported have involved the formation of covalent bonds,[24-27] while others have employed noncovalent interactions.[28-31] Both noncovalent and covalent modifications of the surface have been developed to improve solubility. Noncovalent chemistry includes surfactant modification,[32-34] polymer wrapping[35-36] and polymer absorption[37] in which the polymers were produced by an in situ ring-opening metathesis polymerization or emulsion polymerization. The initial attempts for covalent functionalization took advantage of the higher reactivity of carbon atoms at the ends of the nanotubes to carry out the series of reaction steps leading to the covalent attachment. The oxovanadium(IV) salen Schiff-base loaded on single wall carbon nanotubes (SWNTs) is more suitable as support for the Schiff-base complex than other support like as, high-surface-area activated carbon because the latter exhibits some adventitious activity.[38] Nevertheless, any work in oxovanadium(IV) salen Schiff-bse loaded on MWNTs didn't report.

In the present paper, we have described the preparation of a solid catalyst having a oxovanadium(IV) Schiff-base [VO((OH)$_2$-salen)] complex covalently attached to the MWNTs that is active for the oxidation of cyclohexane. As

far as we know, our report constitutes the first example of MWNTs as support for oxovanadium(IV) salen complex in heterogeneous catalysis.

Experimental

Materials and physical measurements. All other reagents and solvents were purchased from Merck (pro-analysis) and were dried using molecular sieves (Linde 4 Å). Cyclohexane was distilled under nitrogen and stored over molecular sieves (4 Å). Reference samples of cyclohexanol and cyclohexanone were distilled and stored in the refrigerator. XRD patterns were recorded by a Rigaku D-max C III, X-ray diffractometer using Ni-filtered Cu Kα radiation. Transmission electron microscopy (TEM) images were obtained on a Hitachi H-800 transmission electron microscope with an accelerating voltage of 200 kV. FTIR spectra were recorded on Shimadzu Varian 4300 spectrophotometer in KBr pellets. The electronic spectra of the neat complexes were taken on a Shimadzu UV-Vis scanning spectrometer (Model 2101 PC). The stability of the complex covalently attached to the MWNTs was checked after the reaction by UV-Vis and possible leaching of the complex was investigated by UV-Vis in the reaction solution after filtration of the heterogeneous catalyst. The amounts of vanadium complex grafted in MWNTs matrix were determined by the elemental analysis and by subtracting the amount of vanadium complex left in the solutions from the amount taken for the synthesis after the synthesis of the catalysts as determined by UV-Vis spectroscopy. Atomic absorption spectra (AAS) were recorded on a Perkin-Elmer 4100-1319 Spectrophotometer using a flame approach, after acid (HF) dissolution of known amounts of the nanotubes. Diffuse reflectance spectra (DRS) were registered on a Shimadzu UV/3101 PC spectrophotometer the range 1500-200 nm, using MgO as reference. The elemental analysis (carbon, hydrogen and nitrogen) of the materials was obtained from Carlo ERBA Model EA 1108 analyzer. XPS (small area X-ray photoelectron spectroscopy) data were recorded with the PHI-5702 Multi-Technique System, Power Source by Mg Kα line and Ag 3d5/2 FWHM ≤ 0.48 eV. The metal content was measured using inductively coupled plasma (ICP; Labtam 8440 plasmalab) after leaching the metal ions with concentrated nitric acid and very dilute aqueous KOH solution to specific volumes. Thermogravimetric-differential thermal analysis (TG-DTA) was carried out using a thermal gravimetric analysis instrument (Shimadzu TGA-50H) with a flow rate of 20.0 mL min^{-1} and a heating rate of 10 ^{o}C min^{-1}. The products were analyzed by GC-MS on a Philips Pu 4400 gas chromatograph mass spectrometer.

Preparation of *N,N′*-bis(4-hydroxysalicylidene)ethylene-1,2-diamine; H_2[$(OH)_2$-salen]. The stoichiometric amount of 4-hydroxysalicylaldehyde (0.02 mol, 2.76 g) in dissolved methanol (25 mL) is added drop by drop to 1,2-diaminoethane solution (0.01 mol, 0.78 g) in 25 mL methanol. The contents were refluxed for 4 h and a bright yellow precipitate of symmetrical Schiff-base ligand; H_2[$(OH)_2$-salen]; was obtained. The yellow precipitate was separated by filtration, washed and dried in vacuum. It was then recrystalized from methanol to yield H_2[$(OH)_2$-salen]. Yield 97% (1.94 g); orange solid; mp > 230 ^{o}C; IR (KBr, cm^{-1}) $\nu_{C=N}$ 1645. Anal. Calculated for Schiff-base ligand: C, 63.99; H, 5.37; N, 9.33; C/N, 6.86%. Found: C, 63.80; H, 5.20; N, 9.46; C/N, 6.74%. ^{1}H-NMR (DMSO-d_6, ppm) δ 3.76 (s, 4H); 6.14 (d, 2H); 6.24 (dd, 2H); 7.15 (d, 2H); 8.35 (s, 2H); 12.6 (s, 4H).

Preparation of [VO($(OH)_2$-salen)]. The flask containing a stirred suspension of $VOSO_4 \cdot 5H_2O$ (4.05 g, 0.016 mol) in metanol (100 cm^3) was purged with nitrogen, and then warmed to 50 ^{o}C under a nitrogen atmosphere. *N,N′*-bis(4-hydroxysalicylidene)-ethylene-1,2-diamine; H_2[$(OH)_2$-salen]; (4.80 g, 0.016 mol) was added in one portion, and the resulting green suspension was then stirred and heated under reflux and nitrogen atmosphere for 8 h. Then the mixture was cooled and filtered under reduced pressure. The collected solid was washed with diethylether and dried in air to give green crystalline [VO($(OH)_2$-salen)] which was purified by recrystallization from chloroform. Anal. Calculated for [VO($(OH)_2$-salen)]: C, 52.62; H, 3.86; N, 7.67; C/N, 6.86; V, 13.95; V/N, 1.82%. Found: C, 52.47; H, 3.70; N, 7.89; C/N, 6.65; V, 13.80; V/N, 1.74%; IR (KBr, cm^{-1}) $\nu_{C=N}$ 1639.

Multi-wall carbon nanotubes (MWNTs) preparation and purification. Multi-wall carbon nanotubes (MWNTs) used in this study were prepared by chemical vapor deposition (provided by Jiang Youg Trade Co. (China)) with diameters ranging from 20 nm to 40 nm, lengths varying from 1 mm to 10 mm and purity of 85%. The raw product was first immersed in an aqueous solution of HF to remove SiO_2, then filtered and washed with distilled water, and refluxed in diluted HNO_3 for 4 h to remove the metals and amorphous carbon. The resulting solid was then thoroughly washed with deionized water and THF and dried in vacuum. TEM analysis showed that the carbon nanotubes exhibited a multi-wall structure and their diameters were about 20-40 nm.

Chlorination of MWNTs. The purified MWNTs (100 mg) previously dried under vacuum were suspended in a solution of $SOCl_2$ (25 ml) and DMF (1 ml). The suspension was stirred at 65 ^{o}C for 24 h. The solid was then separated by filtration and washed with anhydrous THF, and dried in vacuum.

Anchoring the oxovanadium(IV) salen complex to the MWNTs; [VO($(OH)_2$-salen)]-MWNTs. MWNTs were added (50 mg) to a solution of [VO($(OH)_2$-salen)] (100 mg) in degassed $CHCl_3$ (8 mL), and the suspension was stirred for 20 h under N_2 atmosphere at 70 ^{o}C. The solid was then separated by filtration and exhaustively washed with THF and CH_2Cl_2 and dried in vacuum. The loading of [VO($(OH)_2$-salen)] complex in the MWNTs determined by elemental (N) analysis was 82 μmol g^{-1}. The V content for the oxovanadium(IV) complexes on MWNTs was below the detection limit of quantitative absorption spectroscopy. Anal. Calculated for [VO($(OH)_2$-salen)]-MWNTs: V/N, 1.70%, IR (KBr, cm^{-1}) $\nu_{C=N}$ 1634. Elemental and spectroscopic analysis of [VO($(OH)_2$-salen)] and [VO($(OH)_2$-salen)]-MWNTs confirmed the molecular composition of ligand.

Oxidation of cyclohexane. Aqueous solution of 30%

H_2O_2 (2.27 g, 20 mmol), cyclohexane (0.84 g, 10 mmol) and catalyst (9.2×10^{-5} mol) were mixed in 5 ml of CH_3CN and the reaction mixture was heated at 70 °C with continuous stirring in an oil bath for 2 h. The formation of the reaction products and their identity were confirmed as mentioned above.

Results and Discussion

Synthesis of the oxovanadium(IV) complex was involved heating and stirring of stoichiometric amounts of $H_2[(OH)_2$-salen] and $VOSO_4 \cdot 5H_2O$ in methanol. The desired complex crystallized upon cooling and recrystallized from chloroform. Elemental analysis indicates that the complex is monomeric species formed by coordination of 1 mol of the VO(IV) and 1 mol $H_2[(OH)_2$-salen]. In this study, the metal chelates are insoluble in water but soluble in most organic solvents. Electrical conductivity measurements of the oxovanadium(IV) complex give Λ_M values of 15 Ω^{-1} cm^{-1} mol^{-1} and confirm that they are non-electrolytes. The vanadium content of the MWNTs catalysts were estimated by dissolving the known amounts of the heterogeneous catalyst in concentrated HNO_3 and from these solutions, transition metal contents were estimated by atomic absorption spectrometer. The chemical composition confirmed the purity and stoichiometry of the neat and MWNTs-grafted complex. The chemical analysis of the samples reveals the presence of organic matter with a V/N ratio roughly similar to that of neat complex. The loading of the complex was 82 μmol g^{-1}. The chemical composition confirmed the purity and stoichiometry of the neat and multi-wall carbon nanotubes complexes.

A partial list of IR spectral data has been presented in experimental section. The intensity of the peaks on covalently anchored complex is weak due to their low concentration on MWNTs. The spectra of covalently anchored as well as neat complexes show essentially similar bands. Comparison of the spectra of this catalyst with the ligand provides evidence for the coordinating mode of ligand in catalyst. The ligand exhibits a broad band in the 2450-2750 cm^{-1} due to extensive hydrogen bonding between phenolic hydrogen and nitrogen of azomethine group. Absence of this band in the spectra of covalently anchored complex indicates the destruction of the hydrogen bond followed by the coordination of phenolic oxygen after deprotonation. The sharp band appearing at 1640 cm^{-1} due to ν(C=N) (azomethine), shifts to lower wavenumber and appears at 1635 cm^{-1}. This indicates the involvement of azomethine nitrogen in coordination. The presence of multiple bonds at 2840-2935 cm^{-1} in ligand and its complexes with slight shift suggest the presence of CH_2 group of ethylene in ligand as well as its complexes. Neat complex [VO($(OH)_2$-salen)] exhibits a sharp band at 998 cm^{-1} due to ν(V=O) stretch, while on covalently anchored oxovanadium(IV) complex, location of bands due to ν(V=O) structure, appearance of a strong and broad band at *ca*. 1000 cm^{-1} due to MWNTs framework has not been possible.

The most informative spectroscopic data to support the covalent anchoring of the [VO($(OH)_2$-salen)] complex on

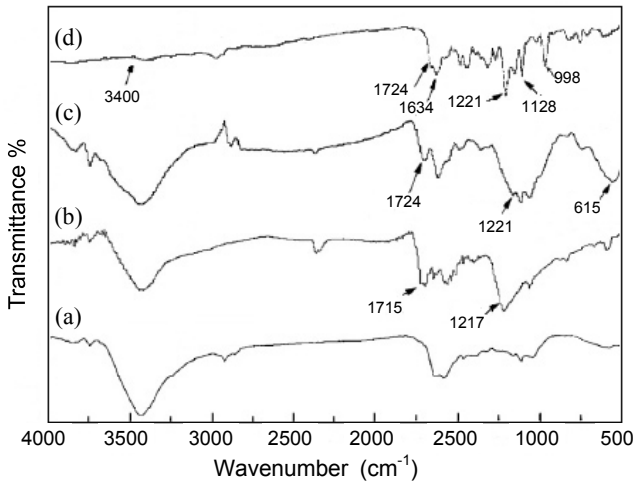

Figure 1. FT-IR spectra of (a) raw MWNTs, (b) HOOC-MWNTs, (c) ClCO-MWNTs, (d) [VO($(OH)_2$-salen)]-MWNTs.

the modified MWNTs were obtained from the comparison of the set of IR corresponding to the raw MWNTs, HOOC-MWNTs and [VO($(OH)_2$-salen)]-MWNTs (Fig. 1). The sharp peak at a: 1519 cm^{-1} in the IR spectrum (a in Fig. 1) is from the stretch mode of the aromatic carbon-carbon bond in raw MWNTs. After the reaction of the shortened MWNTs with $SOCl_2$, the IR spectrum (Fig. 1) showed well defined bands at about 1724, 1221, 615 cm^{-1} which are clearly related to the formation of the group -COCl on the ends and side-wall of MWNTs. The near-IR region of the purified MWNTs was preserved upon functionalization in ClCO-MWNTs and [VO($(OH)_2$-salen)]-MWNTs. this shows that the multi-walled structure of the nanotubes has been preserved unaltered during the treatment (Fig. 1). Metal salen complex exhibits, in the IR, a phenolate stretching vibration band at 1634 cm^{-1} that was proposed as characteristic of this type of complex. Fig. 1 shows the IR spectra recorded for [VO($(OH)_2$-salen)]-MWNTs.

The intensity of the MWNTs-grafted oxovanadium(IV) complex ([VO($(OH)_2$-salen)]-MWNTs) is though weak due to low concentration of the complex, the IR spectra of grafted complex is essentially similar to that of the free metal complex. The adsorbing tendency of the MWNTs might arise from the presence of -COCl on the surface in order to reaction to -OH (Scheme 1).

Furthermore, a control experiment in which a mechanical mixture of MWNTs and 100 μmol g^{-1} of commercial [bis(salicylidene)ethylene-1,2-diimineoxovanadium(IV)]; [VO(salen)]; (no covalent linkage between the complex and MWNTs) was submitted to the extraction procedure with $CHCl_3$ revealed that all the complexes can essentially be recovered by our workup procedure.

The X-ray diffraction patterns of MWNTs contained oxovanadium(IV) complex are similar to MWNTs. This indicates that the crystallinity and morphology of MWNTs were preserved during grafted. Fig. 2 shows XRD pattern of MWNTs, which was similar with that of highly oriented pyrolytic graphite (HOPG). The (002) peak emerged at around 26°, corresponding to the inter-planner spacing of

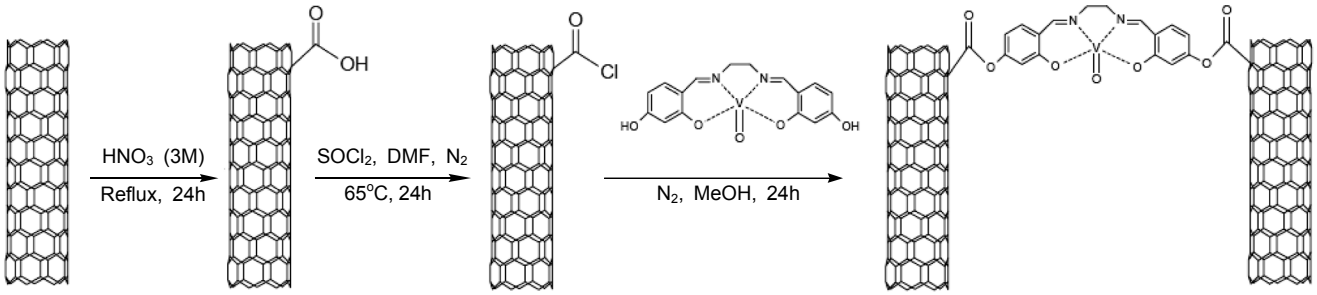

Scheme 1. A drawing of the medication MWNTs by oxovanadium(IV) complex.

0.342 nm, which was a little greater than that of HOPG of about 0.336 nm. Fig. 2 shows XRD patterns of MWNTs with modification grafted method. It could be seen that XRD patterns were similar with raw MWNTs. Modified MWNTs still had the same cylinder wall structure as raw MWNTs and inter-planner spacing of all samples remained the same.

Fig. 3 shows TEM image of MWNTs with high quality, uniform diameter and high length/diameter ratio, which showed that the diameter was about 20-40 nm. From Fig. 3 is found that each MWNTs before modification was mainly a long and folded pipe. MWNTs-Schiff-base complexes exhibit a stretched or folded feature with Schiff-base complex (black dots) mainly congregating in the convex surfaces of MWNTs (Fig. 3). These images of the sample also confirmed the junction formation through Schiff-base complex. As expected, most of the junctions occurred at the tips of the MWNTs, as hydroxyl (OH) groups of the Schiff-base complex react with the carboxylic (COOH) groups in open end of the MWNTs. Scheme 1 illustrates the synthetic step and the structure of the resulting [VO((OH)$_2$-salen)] complex anchored to the MWNTs. According to Fig. 3, in which bundles of MWNTs rather than isolated tubes are seen. In Scheme 1, multi-wall nanotubes represent a simplification of the functionalization process.

MWNTs-Schiff-base complexes enhanced chemical stability and thermal stability in much common solvent. The homogeneous suspension of MWNTs-Schiff-base complex in methanol without any surfactant can be formed by stirring and remains very stable for at least 2 months at room temperature (no breakdown was detected even after high-speed centrifugation or high temperature treatment), while pristine MWNTs are easy to breakdown after high-speed centrifugation or high temperature treatment. The enhanced chemical and thermal stability of MWNTs-Schiff-base complexes might result from covalent interaction between MWNTs and Schiff-base complex. Because Schiff-base complexes were covalently bonded to MWNTs, the strong and super-stable covalent bond interaction between the Schiff-base complexes and MWNTs were responsible for the thermal stability of MWNTs-Schiff-base complexes materials.

The electronic spectral data of ligand and complex have

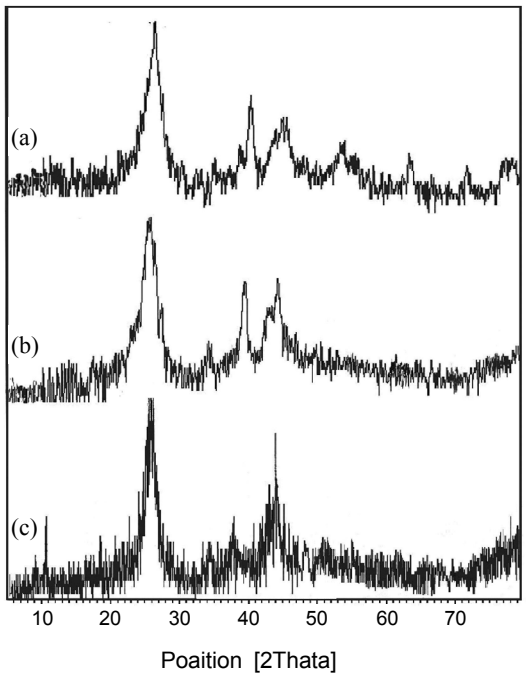

Figure 2. XRD pattern for (a) MWNTs, (b) HOOC-MWNTs, (c) [VO((OH)$_2$-salen)]-MWNTs.

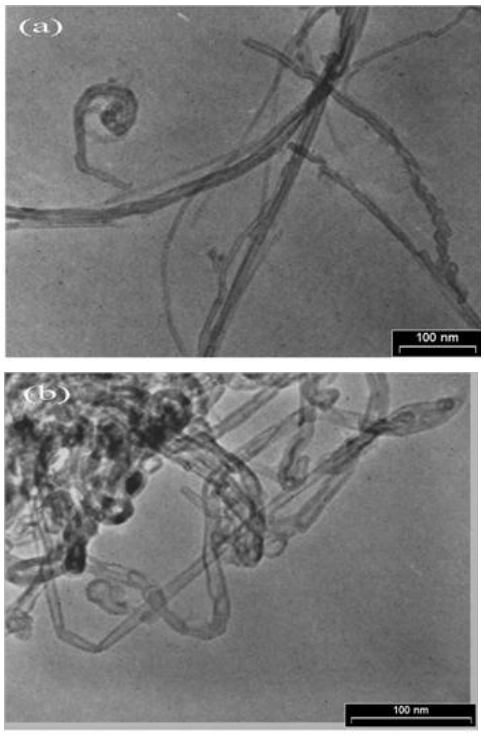

Figure 3. Images TEM of (a) pristine MWNTs, (b) MWNTs functionalized by Schiff-base complex.

also been given in experimental section. The electronic spectral profiles of [VO((OH)$_2$-salen)] and [VO((OH)$_2$-salen)]-MWNTs are reproduced in Fig. 4 and Table 1. The electronic spectrum of ligand H$_2$[(OH)$_2$-salen] exhibits three bands at 335, 265 and 208 nm and these are assigned due to n→π* π→π* and ø→ø* transitions, respectively. All these bands shift to higher wave length side indicating the restructuring of the ligand after coordination to the metal ion. Appearance of a week band due to ligand to metal transition underneath of n→π* transition make this band broad. While no band could be located in further higher wavelength region due to expected d-d transition in the covalently anchored complex; neat complex exhibit at least one broad band at 356 nm in [VO((OH)$_2$-salen)]. On the basis of all these studies, the structures as shown in Scheme 1 have been proposed for this complex, as it was expected for C_{4V} symmetry.[39-40]

Further evidence for the modification of MWNTs coming from the XPS spectrum of [VO((OH)$_2$-salen)]-functionalized MWNTs that could reveal the surface chemical state has been shown in Fig. 5. The peaks at 294.8, 397.8 and 531.1 eV are attributed to C, N and O, respectively.[41] Through calculating the content of elements on surface of MWNTs by area of each element, we can find that the weight content of N is about 2%, indicating the presence of Schiff-base groups. It was found that the O 1s can be fitted to four line shapes with binding energies at 533.1, 532.6, 531.5 and 530.0 eV, which were assigned to VO(IV), -CO-, -C-O-C- and -C-O-VO(IV), respectively. The structure of the complexes could be confirmed (Scheme 1). The XPS spectra related to the core levels of V 2p have been shown in Fig. 5. The peak at 515 eV is attributed to the V 2p3/2. These data confirmed the loading of [VO((OH)$_2$-salen)] complex in the MWNTs.

TGA demonstrates that the composites of [VO((OH)$_2$-salen)]-MWNTs have been prepared (Fig. 6). The mass loss in temperature range below 250 °C reflects the deprotonation of COOH, the loss of acid group of HOOC-MWNTs and humidity. Also the mass loss in this temperature is related to the loss of COCl of MWNTs. On the other hand, Fig. 6 is the TGA curve for the as-prepared MWNTs-Schiff-base complexes, [VO((OH)$_2$-salen)]-MWNTs, which presents several weight losses at the temperature range of 125-400 °C. According to the Fig. 6, decomposition [VO((OH)$_2$-salen)] starts above 250 °C. The significant weight loss of at 250-320 °C is due to the surface grown salen groups. Another weight loss at below 200 °C corresponds to the loss of humidity. No further weight loss can be observed over 480 °C.

Complexes [VO((OH)$_2$-salen)]-MWNTs catalyze the oxidation of cyclohexane by H_2O_2 efficiently to give cyclohexanone, cyclohexanol and cyclohexane-1,2-diol (Table 2). Reaction conditions have also been optimized for the maximum oxidation of cyclohexane by varying different parameters.

Three different 30% aqueous H_2O_2: cyclohexane molar

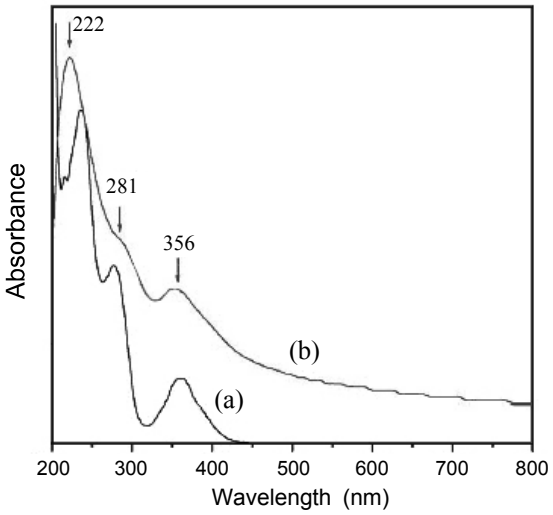

Figure 4. UV-Vis spectra of the (a) [VO((OH)$_2$-salen)]-MWNTs, (b) Schiff-base complex.

Table 1. IR and electronic spectral data of ligand, pure and covalently anchored complex

Compound	IR, cm^{-1}, $\upsilon_{C=N}$	λ_{max}, nm
H$_2$[(OH)$_2$-salen]	1645	208, 265, 335
[VO((OH)$_2$-salen)]	1639	234, 278, 358
[VO((OH)$_2$-salen)]-MWNTs	1634	222, 281, 356

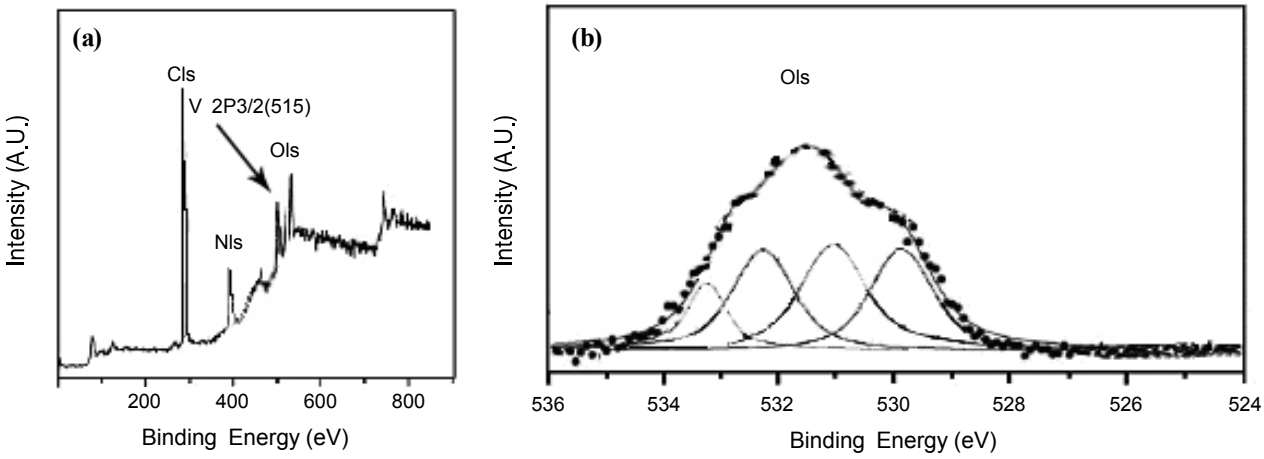

Figure 5. Wide XPS spectrum (a) of [VO((OH)$_2$-salen)] functionalized MWNTs, (b) and curve fitting of the O1s spectrum.

ratios viz. 1:1, 2:1 and 3:1 were considered while keeping the fixed amount of cyclohexane (0.84 g, 10 mmol) and catalyst (9.2×10^{-5} mol) in 5 ml of CH_3CN. The reaction was carried out at 70 °C. The percentage conversions noted at various times have been presented in Fig. 7. A maximum of 67.3% conversion was noted for the H_2O_2 to cyclohexane ratio of 1:1 in 2 h of reaction time. This conversion reached to 78.9% at a H_2O_2 to cyclohexane molar ratio of 2:1. Increasing H_2O_2 to cyclohexane ratio further to 3:1 results in only 60.4% conversion of cyclohexane. This is possibly due to the presence of excess water as has been noted earlier. Thus, a large amount of oxidant is not an essential condition to maximize the oxidation.

The effect of amount of catalyst on the oxidation of cyclohexane has been shown in Fig. 8. Three different amounts of catalyst viz. 3.9×10^{-5} mol, 6.6×10^{-5} mol and 9.2×10^{-5} mol were considered while keeping other conditions as above. It is clear from the plot that 9.2×10^{-5} mol catalyst amount is the best one to obtain the highest cyclohexane conversion. Temperature also has influenced the oxidation of cyclohexane. As shown in Fig. 9, amongst three temperatures of 50, 60 and 70 °C, a maximum conversion of cyclohexane was obtained at 70 °C. Thus, optimized conditions for the oxidation of 10 mmol of cyclohexane are: 9.2×10^{-5} mol catalyst, 20 mmol 30% aqueous H_2O_2, 5 ml CH_3CN and 70 °C reaction temperatures.

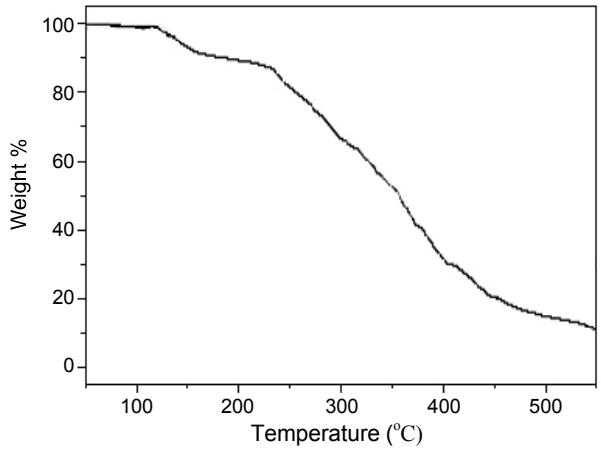

Figure 6. TGA curve of the [VO((OH)$_2$-salen)]-MWNTs

Under these reaction conditions (20 mmol 30% H_2O_2, 9.2×10^{-5} mol catalyst, 5 ml CH_3CN, 10 mmol of cyclohexane, temperature 70 °C), catalyst [VO((OH)$_2$-salen)]-MWNTs gave 78.9% conversion, of cyclohexane with major reaction products of cyclohexanone, cyclohexanol and cyclohexane-1,2-diol as shown in Table 2. About 2 h was required to achieve equilibrium in these reactions. Amongst the various products formed, the selectivity of cyclohexanol was found to be highest while selectivity of other two products were much less. Neat complex has also shown relatively good catalytic activity.

The solid was used as heterogeneous catalyst for the oxidation of cyclohexane (Table 2). One of the major advantages of anchoring the [VO((OH)$_2$-salen)] complex on the MWNTs as support is the ease in which the catalyst can be suspended on the solvent due to the bundled agglomerates of MWNTs that aggregate slowly. Upon initial stirring of the suspension, the black solid remains suspended without setting down for long period of time. This catalyst by higher selectivity and conversion than other catalyst in oxidation reaction sobserved by us.[42-44]

Reusability of the [VO((OH)$_2$-salen)]-MWNTs was confirmed by performing a series of consecutive experiments in

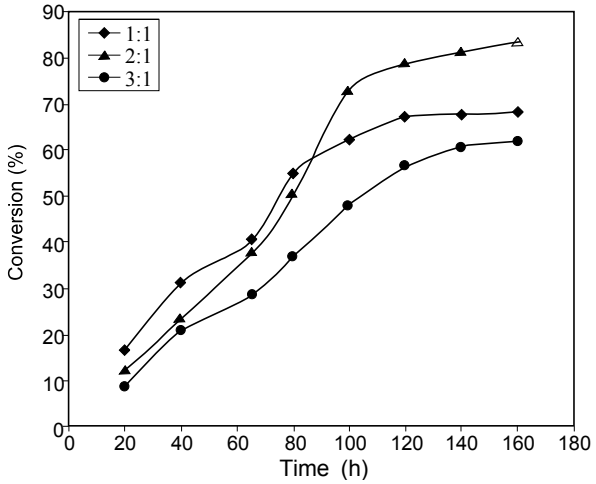

Figure 7. Effect of H_2O_2 concentration on the oxidation of cyclohexane (reaction conditions: 9.2×10^{-5} mol catalyst, 5 ml CH_3CN, temperature 70 °C, catalyst [VO((OH)$_2$-salen)]-MWNTs).

Table 2. Effect of catalyst on the oxidation of cyclohexane and product selectivity.[a]

Catalyst	Conversion (%)	Selectivity (%)		
		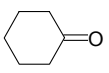	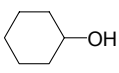	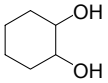
[VO((OH)$_2$-salen)]	42.3	7.3	86.3	6.4
MWNTs	3.1	22.4	55.3	22.3
[VO((OH)$_2$-salen)]-MWNTs	78.9	11.3	79.2	9.5
[VO((OH)$_2$-salen)]-MWNTs[b]	78.3	10.9	79.4	9.7
[VO((OH)$_2$-salen)]-MWNTs[c]	78.1	10.7	79.8	9.5
[VO((OH)$_2$-salen)]-MWNTs[d]	77.5	10.4	80.2	9.4

[a]Reaction condition: 9.2×10^{-5} mol catalyst, 20 mmol 30% H_2O_2, 5 ml CH_3CN, 10 mmol of cyclohexane, temperature 70 °C. [b]First reuse. [c]Second reuse. [d]Third reuse.

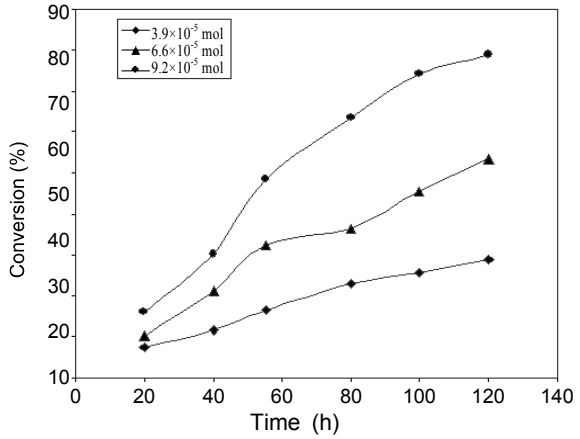

Figure 8. Effect of amount of catalyst on the oxidation of cyclohexane (reaction conditions: 20 mmol 30% H_2O_2, 5 mL CH_3CN, 10 mmol of cyclohexane, temperature 70 °C, catalyst [VO((OH)$_2$-salen)]-MWNTs).

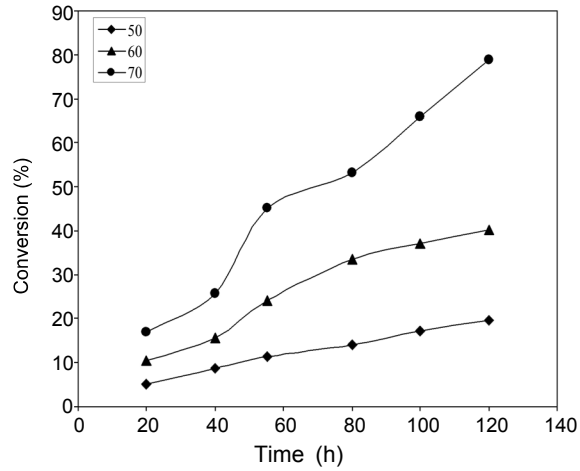

Figure 9. Effect of temperature on the oxidation of cyclohexane (reaction conditions: 9.2×10^{-5} mol catalyst, 20 mmol 30% H_2O_2, 5 mL CH_3CN, 10 mmol of cyclohexane, catalyst [VO((OH)$_2$-salen)]-MWNTs).

which the used catalyst was filtered, washed with fresh solvent, and employed without any further treatment in another run. The results shown in Table 2 clearly prove that no loss of activity occurs, giving a minimum productivity of 300 mol of product per mole of complex.

Conclusion

The MWNTs covalently bonded by oxovanadium(IV) Schiff-base complexes were successfully obtained via the methods of chemical modification. The "neat" and MWNTs covalently anchored oxovanadium(IV) Schiff-base complex exhibit efficient catalytic activity in the oxidation of cyclohexane using H_2O_2. Reaction conditions have been optimized considering different parameters to get maximum conversion of this substrate. A maximum of 78.9% conversion with three different oxidation products of cyclohexane has been obtained with [VO((OH)$_2$-salen)]-MWNTs. The selectivity of these products follows the order: cyclohexanol (79.2%) > cyclohexanone (11.3%) > cyclohexane-1,2-diol (9.5%). This complex is stable and does not leach during the catalytic reaction has been confirmed by testing the filtrate for the corresponding metal ion and thus suggest its heterogeneous nature. The high conversion of the complex makes it suitable catalysts for this catalytic oxidation.

Acknowledgments. Authors are grateful to Council of University of Kashan for providing financial support to undertake this work.

Reference

1. Iijima, S. *Nature* **1991**, *354,* 56.
2. Dresselhaus, M. S.; Dresselhaus, G.; Saito, R. *Carbon* **1995**, *33,* 883.
3. Treacy, M. M.; Ebbesen, T. W.; Gibson, J. M. *Nature* **1996**, *381,* 678.
4. Wong, E. W.; Sheehan, P. E.; Lieber, C. M. *Science* **1997**, *277,* 1971.
5. Falvo, M. R.; Clary, G. J.; Taylor II, R. M.; Chi, V.; Brooks Jr., F. P.; Washburn, S.; Superfine, R. *Nature* **1997**, *389,* 582.
6. de Heer, W. A.; Chatelain, A.; Ugarte, D. *Science* **1995**, *270,* 1179.
7. Dai, H.; Wong, E. W.; Lieber, C. M. *Science* **1996**, *272,* 523.
8. Nakamura, T.; Ohana, T.; Ishihara, M.; Hasegawa, M.; Koga, Y. *Diamond and Related Materials* **2007**, *16,* 1091.
9. Showkat, A. M.; Lee, K.-P.; Gopalan, A. I.; Choic, S.-H.; Nho, Y. C. *Diamond and Related Materials* **2007**, *16,* 1688.
10. Kokai, D. F.; Koshio, A.; Shiraishi, M.; Matsuta, T.; Shimoda, S.; Ishihara, M.; Koga, Y.; Deno, H.; *Diamond and Related Materials* **2005**, *14,* 724.
11. Ebbesen, T. W.; Lezec, H. J.; Hiura, H.; Bennett, J. W.; Ghaemi, H. F.; Thio, T. *Nature* **1996**, *382,* 54.
12. Wildöer, J. W.; Venema, L. C.; Rinzler, A. G.; Smalley, R. E.; Dekker, C. *Nature* **1998**, *391,* 59.
13. Li, Y. B.; Wei, B. Q.; Liang, J.; Yu, Q.; Wu, D. H. *Carbon* **1999**, *37,* 493.
14. Kim, Y. A.; Hayashi, T.; Fukai, Y.; Endo, M.; Yanahisawa, T.; Dresselhaus, M. S. *Chem. Phys. Lett.* **2002**, *355,* 279.
15. Shelimov, K. B.; Esenaliev, R. O.; Rinzler, A. G.; Huffman, C. B.; Smalley, R. E. *Chem. Phys. Lett.* **1998**, *282,* 429.
16. Hilding, J.; Grulke, E. A.; Zhang, Z. G.; Lockwood, F. J. *Dispersion Sci. Technol.* **2003**, *24,* 1.
17. Riggs, J. E.; Walker, D. B.; Carroll, D. L.; Sun, Y. P. *J. Phys. Chem. B* **2000**, *104,* 7071.
18. Matarredona, O.; Rhoads, H.; Li, Z.; Harwell, J.; Balzano, L.; Resasco, D. *J. Phys. Chem. B* **2003**, *107,* 13357.
19. Chiu, P. W.; Duesberg, G. S.; Dettlaff-Weglikowska, U.; Roth, S. *Appl. Phys. Lett.* **2002**, *80,* 3811.
20. Chen, J.; Hamon, M. A.; Hu, H.; Chen, Y.; Rao, A. M.; Eklund, P. C.; Haddon, R. C. *Science* **1998**, *282,* 95.
21. Mickelson, E. T.; Chiang, I. W.; Zimmerman, J. L.; Boul, P. J.; Lozano, J.; Liu, J.; Smalley, R. E.; Hauge, R. H.; Margrave, J. L. *J. Phys. Chem. B* **1999**, *103,* 4318.
22. Lau, K. T.; Hui, D. *Carbon* **2002**, *40,* 1605.
23. Garg, A.; Sinnott, S. B. *Chem. Phys. Lett.* **1998**, *295,* 273.
24. Bahr, J. L.; Yang, J.; Kosynkin, D. M.; Bronikowski, M. J.; Smalley, R. E.; Tour, J. M. *J. Am. Chem. Soc.* **2001**, *123,* 6536.
25. Pompeo, F.; Reasaco, D. *Nano Lett.* **2002**, *2,* 369.
26. Dyke, C. A.; Tour, J. M. *Nano Lett.* **2003**, *3,* 1215.
27. Strano, M. S.; Dyke, C. A.; Usrey, M. L.; Barone, P. W.; Allen, M. J.; Shan, H.; Kittrell, C.; Hauge, R. H.; Tour, J. M.; Smalley, R. E. *Science* **2003**, *301,* 1519.
28. Chen, J.; Rao, A. M.; Lyuksyutov, S.; Itkis, M. E.; Hamon, M. A.; Hu, H.; Cohn, R. W.; Eklund, P. C.; Colbert, D. T.; Smalley, R. E.; Haddon, R. C. *J. Phys. Chem. B* **2001**, *105,* 2525.

29. O'Connell, M. C.; Boul, P.; Ericson, L. M.; Huffman, C.; Wang, Y.; Haroz, E.; Kuper, C.; Tour, J.; Ausman, K. D.; Smalley, R. E. *Chem. Phys. Lett.* **2001**, *342,* 265.
30. Chattopadhyay, D.; Lastella, S.; Kim, S.; Papadimitrikapoulos, F. *J. Am. Chem. Soc.* **2002**, *124,* 728.
31. Chattopadhyay, D.; Galeska, I.; Papadimitrikapoulos, F. *J. Am. Chem. Soc.* **2003**, *125,* 3370.
32. O'Connell, M. J.; Bachilo, S. M.; Huffman, C. B.; Moore, V. C.; Strano, M. S.; Haroz, E. H.; Rialon, K. L.; Boul, P. J.; Noon, W. H.; Kittrell, C.; Ma, J. P.; Hauge, R. H.; Weisman, R. B.; Smalley, R. E. *Science* **2002**, *297,* 593.
33. Islam, M. F.; Rojas, E.; Bergey, D. M.; Johnson, A. T.; Yodh, A. G. *Nano Lett.* **2003**, *3,* 269.
34. Kang, Y. J.; Taton, T. A. *J. Am. Chem. Soc.* **2003**, *125,* 5650.
35. Star, A.; Stoddart, J. F. *Macromolecules* **2002**, *35,* 7516.
36. Star, A.; Stoddart, J. F.; Steuerman, D.; Diehl, M.; Boukai, A.; Wong, E. W.; Yang, X.; Chung, S. W.; Choi, H.; Heath, J. R. *Angew. Chem., Int. Ed.* **2001**, *40,* 1721.
37. Ballhausen, C. J.; Gray, H. B. *Molecular Orbital Theory*; Benjamin: New York, 1965.
38. Baleizão, C.; Gigante, B.; Garcia, H.; Corma, A. *J. Catal.* **2004**, *221,* 77.
39. Salavati-Niasari, M.; Elzami, M. R.; Mansournia, M. R.; Hydarzadeh, S. *J. Mol. Catal. A: Chem.* **2004**, *221,* 169.
40. Lever, A. B. P. *Crystal Field Spectra. Inorganic Electronic Spectroscopy,* lst ed.; Elsevier: Amsterdam, 1968; p 249.
41. Cui, J.; Wang, W. P.; You, Y. Z.; Liu, C.; Wang, P. *Polymer* **2004**, *45,* 8717.
42. Salavati-Niasari, M.; Sobhani, A. *J. Mol. Catal. A: Chem.* **2008**, *285,* 58.
43. Salavati-Niasari, M. *Microporous Mesoporous Mater.* **2006**, *92,* 173.
44. Salavati-Niasari, M.; bazarganipour, M. *J. Mol. Catal. A: Chem.* **2007**, *278,* 17.